



# Design, fabrication and measurement of highly-dispersive mirrors with total internal reflection

PENGHUI MA,<sup>1,\*</sup> YU CHEN,<sup>2</sup> TATIANA AMOTCHKINA,<sup>2</sup> MICHAEL TRUBETSKOV,<sup>2</sup>  VLADIMIR PERVAK,<sup>3</sup> AND LI LI<sup>1</sup>

<sup>1</sup>National Research Council Canada, 1200 Montreal Rd. Ottawa, Ontario, Canada

<sup>2</sup>Max-Planck-Institut für Quantenoptik, Hans-Kopfermann-Str. 1, 85748, Garching, Germany

<sup>3</sup>Ludwig Maximilians University, Am Coulombwall 1, 85748, Garching, Germany

\*penghui.ma@nrc-cnrc.gc.ca

**Abstract:** High group delay dispersion (GDD) is often required for ultrafast laser applications. To achieve GDD level higher than  $-10000 \text{ fs}^2$  in a single mirror setting is difficult due to the high sensitivity to unavoidable production inaccuracies. To overcome the problem, total internal reflection (TIR) based dispersive mirrors have been proposed in theory. In this paper, we report our continuous effort to further design, fabricate and measure TIR based dispersive mirrors.

© 2020 Optical Society of America under the terms of the [OSA Open Access Publishing Agreement](#)

## 1. Introduction

Thin film interference based dispersive mirrors (DM) are critical optical components that have found wide applications for pulse control or shaping in ultrafast lasers [1–8]. Compared to other pulse shaping devices such as prisms or gratings, DMs have the advantage of resulting in simpler and more efficient laser systems. For some ultrafast laser applications, a large GDD is often required [9]. For example, in the high-power mode-locking laser with a thin-disk as described in Ref. [10], the roundtrip GDD about  $-346500 \text{ fs}^2$  in the laser system was needed to compensate the large phase shift introduced by self-phase modulation. However, it is usually difficult to obtain a GDD level higher than  $-5000 \text{ fs}^2$  in a single DM [1]. As a result, multiple DMs in combination with multiple bounces often have to be implemented in a complicated arrangement in order to achieve such a high GDD level. For example, six DMs with GDD of  $-2500 \text{ fs}^2$  or less were used in [10].

Clearly, it would be desirable to use fewer numbers of DMs to simplify the lasers systems if the GDD level of a single DM could be increased. In a recent publication, a new level of GDD in the order of  $-10000 \text{ fs}^2$  was achieved for thin film based DMs in the wavelength region from 1025 nm to 1035 nm [11]. The mirror coating is made of  $\text{SiO}_2$  and  $\text{Ta}_2\text{O}_5$  and consists of 50 layers with a total layer thickness of  $13.7 \mu\text{m}$ . However, it is very challenging to further increase the GDD level of a single DM for similar DM designs. For example, to increase the GDD level from  $-10000 \text{ fs}^2$  to  $-20000 \text{ fs}^2$ , the number of layers and the total layer thicknesses would be even bigger and thus make it much more difficult to fabricate.

In an effort to increase the GDD level of a single DM, and at the same time, to keep the number of layers and the total layer thickness low, total internal reflection (TIR) has been proposed to be combined with thin film interference to design new highly dispersive DM with GDDs in the range of  $-15000 \text{ fs}^2$  to  $-20000 \text{ fs}^2$  [12]. In this case, light is incident on the DM from a high index substrate and the incident angle is larger than the critical angle. The advantage of using TIR is that the mirror automatically has 100% reflection and thus it only needs to meet the GDD requirement. As a result, it is possible to simplify the layer design and achieve high GDD simultaneously. To date, no practical DMs based on TIR have been fabricated. It is therefore

the objective of the paper to further investigate the factors in the design of TIR based DMs, to fabricate and measure the performance of such TIR DMs.

In this paper, we report a fabricated TIR DM with a measured GDD of  $-15000 \text{ fs}^2$  at wavelength from 795 nm to 805 nm. In Section 2, we give detailed description about the TIR DM design. The fabrication of the TIR DMs can be found in Section 3. In section 4, customized GDD measurements are described. Finally, conclusions are given in Section 5.

## 2. Design of DMs in TIR configuration

### 2.1. Advantages of TIR DMs

In a simple TIR DM configuration with a  $45^\circ$  right-angle prism as shown in Fig. 1, the mirror coating is deposited onto the hypotenuse surface of the prism. AR coatings are applied on the entrance and exit surface of the prism. There is GDD contribution associated with transmission through the AR coatings. However, these contributions are very small. For example, a 5-layer AR coating has transmission GDD less than  $0.2 \text{ fs}^2$ . The prism has higher index than that of the exit medium, in this case, it is air. Since the angle of incidence (AOI) is larger than the critical angle at the DM and the air interface, thus, total internal reflection occurs. One advantage of having the TIR configuration is that it automatically satisfies the high reflection requirement of a DM. During the DM design process, a thin film synthesis program only needs to meet the dispersion related GDD targets while searching and optimizing different mirror designs. As such, it can generally result in less complicated multilayer structure compared to the cases where both reflectance and dispersion are targeted as in conventional DMs that operate at normal or small angles of incidence.

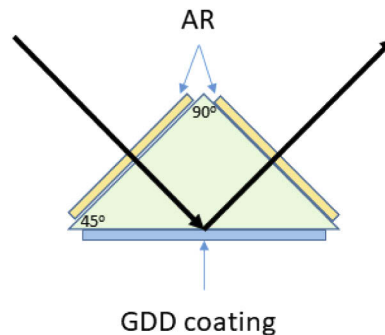


**Fig. 1.** A simple TIR DM configuration with a right angle prism. The prism has refractive index such that its critical angle to air is smaller than  $45^\circ$ .

In a multilayer with high  $n_H$  and low  $n_L$  refractive index materials, it is commonly known that a higher index contrast  $n_H/n_L$  can often lead to simpler multilayer structure for given design targets. In the case of optical coatings operate at oblique angles of incidence (TIR DMs fall in this category), the index contrast is replaced by the admittance ratio  $\eta_H/\eta_L$  [13,14]. Although TIR DMs can be designed for either s- or p-polarized light as seen in [12], it is s-polarized light that has advantage on admittance contrast. We define the index ratio factor  $F$  as

$$F \equiv \left( \frac{n_H^S}{\eta_L^S} \right) / \left( \frac{n_H}{n_L} \right). \quad (1)$$

$F$  is simply the ratio of index contrasts between oblique angle of incidence and normal incidence. If it is larger than 1, the multilayer has higher index contrast at oblique incidence than at normal

incidence.  $F$  can be expressed as a function of angle of incidence ( $\theta_0$ ) and index of entrance medium ( $n_0$ ). For s-polarized light,

$$F = \frac{\sqrt{1 - \left(\frac{n_0 \sin \theta_0}{n_H}\right)^2}}{\sqrt{1 - \left(\frac{n_0 \sin \theta_0}{n_L}\right)^2}}. \quad (2)$$

As long as  $F$  is real (i.e. no absorption and frustrated total internal reflection in the layers),  $F$  for s-polarized light is always larger than or equal to 1 and it is also monotonically increases with  $\theta_0$ . In other words, higher  $n_0 \sin \theta_0$  results in higher multilayer index contrast for s polarization.

As an example, Fig. 2 plots  $F$  as a function of  $\theta_0$  for a multilayer with fused silica as incident medium,  $\text{SiO}_2$  and  $\text{Nb}_2\text{O}_5$  as low and high index layers, respectively. At  $\theta_0 = 45^\circ$ ,  $F = 1.35$ . This is already a substantial increase in index contrast for s-polarization in comparison to normal incidence.

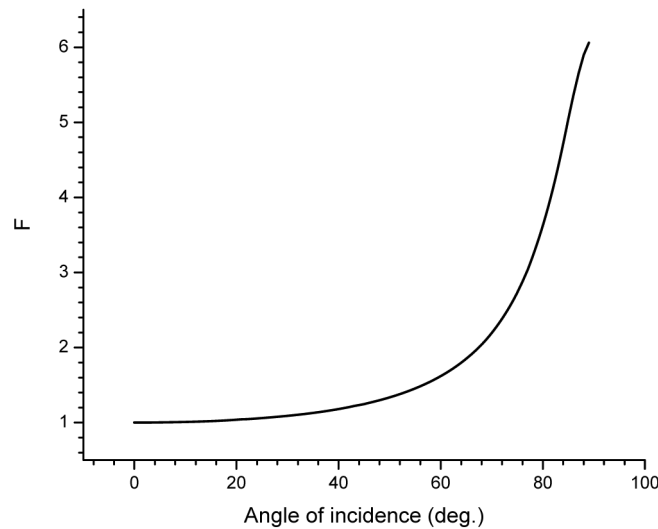


**Fig. 2.** Index ratio factor  $F$  as a function of angle of incidence in incident medium. The layer materials are  $\text{SiO}_2$  and  $\text{Nb}_2\text{O}_5$  and the incidence medium is fused silica

## 2.2. Highly dispersive DMs in TIR configurations

To demonstrate the influence of angle of incidence on the performance of TIR DMs for s-polarized light, we have designed a series of highly dispersive DMs. The GDD target is  $-15000 \text{ fs}^2$  between 795 and 805 nm.  $\text{SiO}_2$  and  $\text{Nb}_2\text{O}_5$ , are used as layer materials. The material of the prism is fused silica. The designed TIR DMs have AOI from  $45^\circ$  to  $85^\circ$ . For comparison, a mirror for normal incidence is also designed with a minimum reflectance of 99.65%. All the mirrors are designed using commercial software OptiLayer [15]. The gradual evolution searching was stopped when the same merit function is reached for all the designs and there was no manual intervention during the search. The GDD performances of four mirrors are plotted in Fig. 3. As can be seen, all performances are quite similar for different AOIs, particularly on the specified wavelength range. The parameters of the different DM designs are listed in Table 1. We can see that number of layers substantially reduced in TIR configurations in compared to normal incidence. Consistent with predictions of last subsection, the number of layers decreases with angle of incidence, meaning simpler multilayer structure for higher AOI.

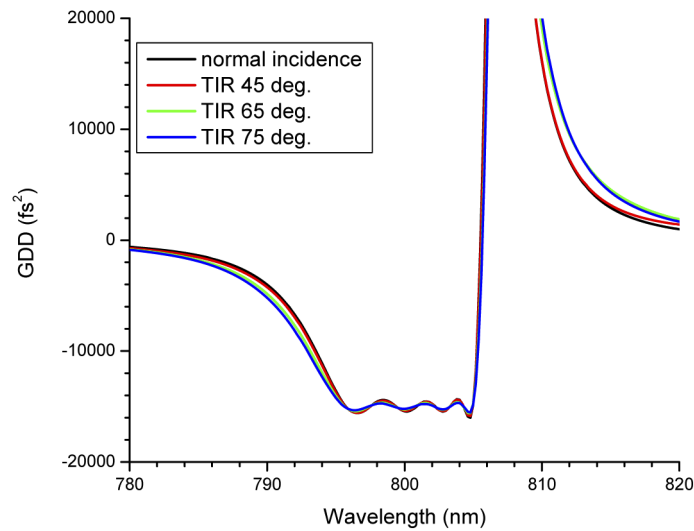


**Fig. 3.** Reflected GDD for s-pol of the TIR mirrors at different angles of incidence.

**Table 1. Parameters of different TIR DM designs**

Design	AOI (°)	R <sub>min</sub>	# of Layers	Physical thickness (μm)	F
1	0	99.65%	81	10.44	1
2	45	TIR	49	6.67	1.35
3	55	TIR	43	7.67	1.58
4	65	TIR	33	6.93	2.02
5	75	TIR	23	8.78	3.00
6	85	TIR	19	10.83	5.54

However, at very high AOI, more physical thickness is needed. This is due to the cosine factor in the optical phase of a layer:

$$\varphi = \frac{2\pi n d \cos\theta}{\lambda}. \quad (3)$$

The higher AOI, the smaller the cosine factor is, and therefore need more physical thickness for a specified optical phase. At very high AOI, the need for more physical thickness becomes much significant. It appears that for these particular DMs, the most economic AOI in terms of physical thickness is between 45° and 65°.

### 3. Manufacture of the TIR DM

The fabricated DM has the same configuration as shown in Fig. 1. For laser applications, laser beam usually has a small divergence. To account for this divergence, the multilayer design targets include  $\pm 0.35^\circ$  angular tolerance inside the prism and about  $\pm 0.5^\circ$  tolerance in air. The GDD specs are again  $-15000 \text{ fs}^2$  on wavelengths in range [795,805] nm. Light travels inside the prism for about 10 mm since the length of the silica prism leg is 10 mm. The resulting positive GDD from silica is a few hundred  $\text{fs}^2$  and quite small compared to the designed target of  $-15000 \text{ fs}^2$ . The design procedure is a typical numerical one. Design software generates potential designs, and then the designer manually adjusts and reoptimize the multilayer structure. The designer's intervention can often further simplify the multilayer and make it more suitable for manufacture than automatically generated ones. The final design has 41 layers of  $\text{SiO}_2$  and  $\text{Nb}_2\text{O}_5$  and the

total physical thickness is 6.56  $\mu\text{m}$ . The index profile of this design is shown in Fig. 4(a) and the GDD performances at three different angles of incidence are plotted in Fig. 4(b).

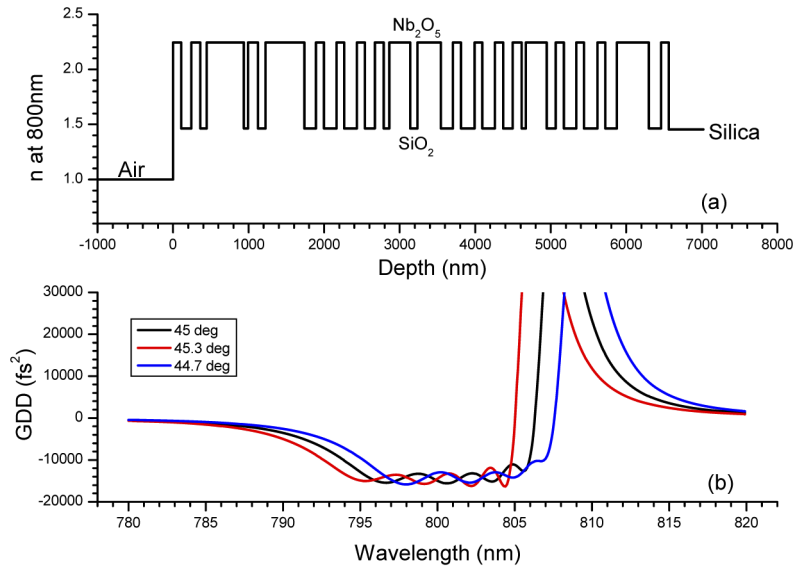


**Fig. 4.** (a) Design profile of the dispersive multilayer at 800 nm. (b) Reflected GDD for S-pol of the DM at three angles of incidence.

Before the actual coating deposition, a simple layer-thickness Monte-Carlo simulation [15] was carried out on the TIR design and the conventional normal incidence design. The 66.7% success corridors for 0.2nm random error on layer thickness are plotted in Fig. 5. The relatively narrower corridor for TIR design due to simpler multilayer structure means TIR has much better chance made to meet the design target. However, on the abstract values of the corridor width particularly at higher wavelengths, one can conclude that even the TIR design is challenging to make. These DM's are less likely to be made close to target if the coating strategy is based on layer thickness determination only. Additional measure, such as reoptimization of multilayer during the coating process, is necessary to overcome the high thickness sensitivity.

The TIR DM coating was deposited in a dual magnetron sputtering system. This system is very stable and has been used to fabricate many challenging multilayer filters [16,17].  $\text{SiO}_2$  and  $\text{Nb}_2\text{O}_5$  layers were deposited by reactive sputtering of Si and Nb targets in Ar and  $\text{O}_2$  mixture respectively. The refractive indices of these two sputtered materials can be accurately described with a Cauchy dispersive model between 420 and 1200nm. The model parameters are

	A	B	C
$\text{SiO}_2$	1.4591	0.0035	0.0000
$\text{Nb}_2\text{O}_5$	2.1903	0.0304	0.0025

The magnetron sputtering system has a broadband optical monitoring which is capable to measure transmittance of a witness slide located closely to the prism having the actual DM coating. The transmittance on the witness slide was measured after the completion of each layer and the layer thickness was determined afterwards by fitting calculated transmittance to the measured values. The thicknesses on the prism were calculated using a calibrated tooling factor. In case a difference between the desired and determined thicknesses is detected, the remaining

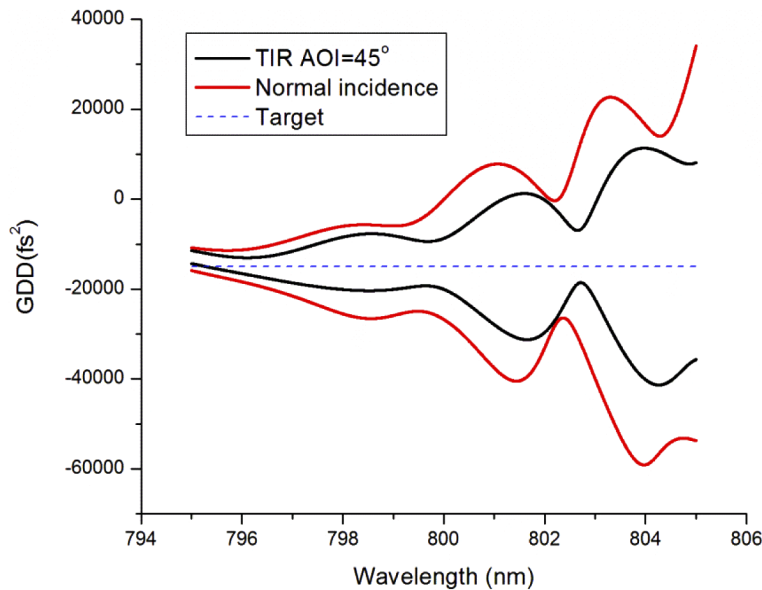


**Fig. 5.** 66.7% success corridors for 45° TIR and conventional normal incidence DMs. The random error on layer thickness is 0.2 nm.

layers are reoptimized so that adversary effect of the previous thickness error is compensated or partially compensated. This dynamic deposition strategy is particularly suitable for very complicated multilayer deposition such as the TIR DMs.

### 3.1. Post deposition measurements

The fabricated TIR(45°) DM was carefully measured to ensure the desired performance is achieved. The first measurements were obtained using a variable angle spectral ellipsometer. These are indirect measurements for a DM. However, ellipsometry can often be measured with very high accuracy and therefore is a good indication to the deposition accuracy. The measurements were carried out at the both side of the dispersive multilayer, i.e. inside the prism and on the air side. The measured ellipsometry data are plotted in Fig. 5 with circles for  $\Psi$  and triangles for  $\Delta$ . The lines are the calculated quantities using layer thicknesses determined during the coating run. We see in both measurements the calculations match to the measured data very well indicating high accuracy of coating fabrication.

## 4. GDD measurements of TIR DM

The standard white light interferometer (WLI) setup [18] was adjusted specially to measure the dispersive prism optical element under consideration. A schematic of the WLI is presented in Fig. 7.

A fiber-transmitted white light passes into the interferometer. After propagation through a polarizer, the incoming p-polarized collimated beam was divided by a beam splitter cube (BS) into two interferometer arms: sample and reference ones. The prism was placed into the sample arm. The length of the sample arm was accurately adjusted in order to provide overlapping the beams propagating in the sample and reference arms, i.e.  $d_R = d_S + d_1 + d_2$ . The length of the reference arm was finally adjusted by careful moving the Ag-mirror to get a stable interference pattern between beams coming from two arms and to achieve maximum contrast of interference fringes. During the measurement process, the reference arm was moved by a stepper motor that

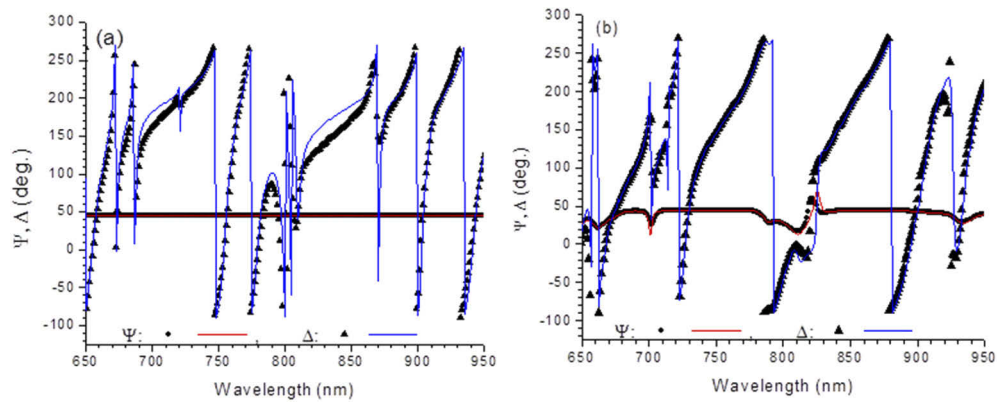


**Fig. 6.** Ellipsometry measurements of the multilayer. Circles: measured  $\Psi$ , triangles: measured  $\Delta$ , and lines: calculated quantities. (a) for measurement inside the prism with  $\text{AOI}=45^\circ$ . (b) for measurement on the air side with  $\text{AOI}=70^\circ$ .

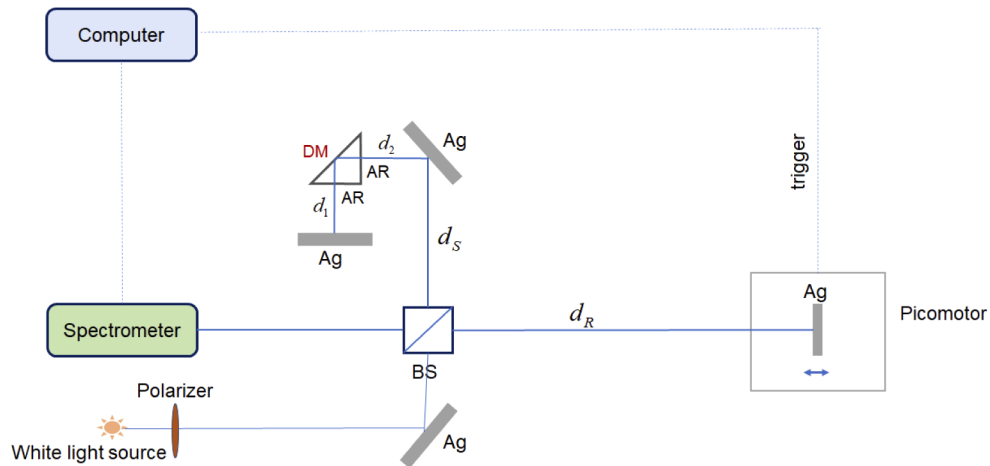


**Fig. 7.** WLI measurement set-up

drives a precision linear translation stage. The motor makes 25 steps per second with a step size of 20–30 nm. The total scanning time is approximately 10 min. One spectral scan is taken at every step of the motor that moves the silver mirror at the end of reference arm. The overlapped beams are passed by another fiber to a grating spectrometer with a CCD camera. The exposure time of the CCD camera in spectrometer is less than the interval between adjacent motor steps. During the scanning time, 12000 spectral scans were recorded. The wavelength grid consists of 1340 spectral points in the spectral range 683–909 nm providing the spectral resolution of 0.17 nm. All elements of the WLI are placed on a high-quality optical table, reducing vibrations to an acceptable level. The level of errors in intensity values caused by light-source noise and detector noise can be estimated at 3%. As a result of the described measurement process, a two-dimensional array of data containing  $1340 \times 12000$  points were obtained and stored at the computer.

GD and GDD in the spectral region of interest were extracted using specially developed algorithm [18]. The algorithm keeps the initial spectral resolution of 0.17 nm that is important to describe so challenging GD features in the designed optical element.

The measured GD and GDD and the calculated ones are plotted in Fig. 8. As can be seen in Fig. 8(a), the correspondence between measured GD and calculated GD is quite good. There are some deviations caused by (i) manufacturing errors inevitable in all deposition plants (ii) measurement errors. Extraction of GDD data is more complicated since this is derivative from GD that is calculated based on measurement data. Calculation of such a derivative is performed using a special algorithm that uses a smoothing procedure of GD. The correspondence between measurement GD and the calculated and even GDD and the calculated is good enough if we take the design sensitivity into account.

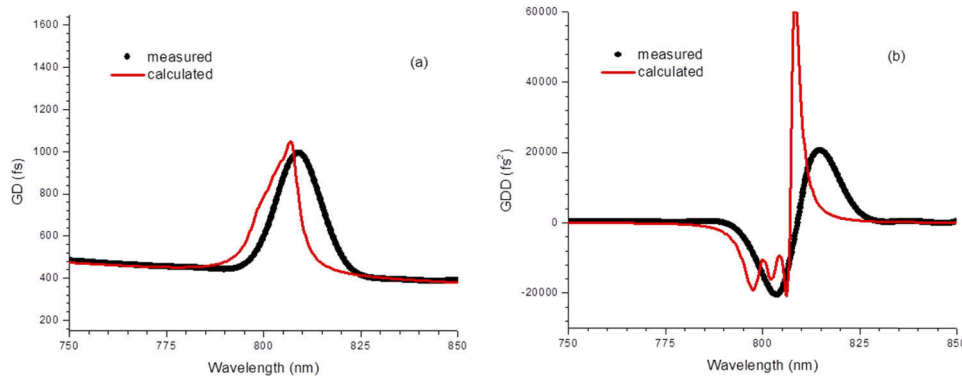


**Fig. 8.** (a) Measured and calculated GD. GD for 10 mm travel inside silica and an arbitrary constant offset are added to the calculated GD to match the measured data. (b) Measured and calculated GDD.

## 5. Conclusion

We have demonstrated that highly dispersive TIR DMs can be designed, fabricated, and measured. We have shown such DMs can have much simpler layer structures than conventional DMs operating at normal or small angles of incidences. With a 41-layer mirror design and a total layer thickness of only 6.7  $\mu\text{m}$ , a TIR DM has been achieved a GDD value of  $-15000 \text{ fs}^2$ . Such TIR dispersive mirrors could provide alternative solution for ultrafast lasers that require high GDDs and thus significantly simplify the laser systems. As described in section 2.1, the advantages of this new TRI DM are not wavelength dependent. Although the TIR configuration and coatings demonstrated in this paper are for wavelengths around 800nm, with similar advantages, it can be readily applied to nearby wavelengths or any wavelengths where proper materials exist. Other TIR DMs with different GDD or layouts will be investigated in future developments

## Disclosures

The authors declare no conflicts of interest.

## References

1. R. Szípcos and A. Koházi-Kis, "Theory and design of chirped dielectric laser mirrors," *Appl. Phys. B: Lasers Opt.* **65**(2), 115–135 (1997).
2. V. Pervak, "Optical coatings for high-intensity femtosecond lasers," in *Optical Thin Films and Coatings: From Materials to Applications* (Elsevier Ltd, 2013), pp. 664–694.
3. R. Szípcos, K. Ferencz, C. Spielmann, and F. Krausz, "Chirped multilayer coatings for broadband dispersion control in femtosecond lasers," *Opt. Lett.* **19**(3), 201–203 (1994).
4. V. Pervak, I. Ahmad, S. A. Trushin, Z. Major, A. Apolonski, S. Karsch, and F. Krausz, "Chirped-pulse amplification of laser pulses with dispersive mirrors," *Opt. Express* **17**(21), 19204–19212 (2009).
5. P. Dombi, P. Rácz, M. Lenner, V. Pervak, and F. Krausz, "Dispersion management in femtosecond laser oscillators with highly dispersive mirrors," *Opt. Express* **17**(22), 20598–20604 (2009).

6. O. Pronin, J. Brons, C. Grasse, V. Pervak, G. Boehm, M.-C. Amann, A. Apolonski, V. L. Kalashnikov, and F. Krausz, "High-power Kerr-lens mode-locked Yb:YAG thin-disk oscillator in the positive dispersion regime," *Opt. Lett.* **37**(17), 3543–3545 (2012).
7. Y. Chen, Y. Wang, L. Wang, M. Zhu, H. Qi, J. Shao, X. Huang, S. Yang, C. Li, K. Zhou, and Q. Zhu, "High dispersive mirrors for erbium-doped fiber chirped pulse amplification system," *Opt. Express* **24**(17), 19835–19840 (2016).
8. T. Amotchkina, M. Trubetskov, S. Hussain, D. Hahner, D. Gerz, M. Huber, W. Schweinberger, I. Pupeza, F. Krausz, and V. Pervak, "Broadband dispersive Ge/YbF<sub>3</sub> mirrors for mid-infrared spectral range," *Opt. Lett.* **44**(21), 5210–5213 (2019).
9. V. Pervak, O. Pronin, O. Razskazovskaya, J. Brons, I. B. Angelov, M. K. Trubetskov, A. V. Tikhonravov, and F. Krausz, "High-dispersive mirrors for high power applications," *Opt. Express* **20**(4), 4503–4508 (2012).
10. D. Bauer, I. Zawischa, D. H. Sutter, A. Killi, and T. Dekorsy, "Mode-locked Yb:YAG thin-disk oscillator with 41  $\mu$ J pulse energy at 145 W average infrared power and high power frequency conversion," *Opt. Express* **20**(9), 9698–9704 (2012).
11. E. Fedulova, K. Fritsch, J. Brons, O. Pronin, T. Amotchkina, M. Trubetskov, F. Krausz, and V. Pervak, "Highly dispersive mirrors reach new levels of dispersion," *Opt. Express* **23**(11), 13788–13793 (2015).
12. Li Li, "Highly Dispersive Chirped Mirror Designs with Total Internal Reflection," in *Optical Interference Coatings*, (Optical Society of America, 2016), TD4;
13. H. A. Macleod, *Thin-Film Optical Filters*, 5th edition (CRC, 2017)
14. P. W. Baumeister, *Optical Coating Technology*, (SPIE, 2004)
15. A. V. Tikhonravov and M. K. Trubetskov, OptiLayer Thin Film Software, <http://www.optilayer.com>
16. Penghui Ma, L. Li, F. Lin, and J. A. Dobrowolski, "Manufacture of high performance polarizing beam splitter for projection display applications," in *Optical Interference Coatings*, (Optical Society of America, 2007), TuC1.
17. P. Ma, F. Lin, and J. A. Dobrowolski, "Design and manufacture of metal/dielectric long-wavelength cutoff filters," *Appl. Opt.* **50**(9), C201–C209 (2011).
18. T. Amotchkina, A. Tikhonravov, M. Trubetskov, D. Grupe, A. Apolonski, and V. Pervak, "Measurement of group delay of dispersive mirrors with white-light interferometer," *Appl. Opt.* **48**(5), 949–956 (2009).